Temperature Dependence of the Fundamental Bandgap of InN

J. Wu, W. Walukiewicz, W. Shan, K.M. Yu, J.W. Ager III,
Materials Sciences Division, Lawrence Berkeley National Laboratory,
Berkeley, California 94720,
S. X. Li, E.E. Haller,
Department of Materials Science and Engineering, University of California, Berkeley,
and Materials Sciences Division, Lawrence Berkeley National Laboratory,
Berkeley, California 94720,
Hai Lu, and William J. Schaff,
Department of Electrical and Computer Engineering, Cornell University, Ithaca, New York 14853

The fundamental bandgap of InN films grown by molecular beam epitaxy have been measured by transmission and photoluminescence spectroscopy as a function of temperature. The band edge absorption energy and its temperature dependence depend on the doping level. The bandgap variation and Varshni parameters of InN are compared with other group III-nitrides. The energy of the photoluminescence peak is affected by the emission from localized states and cannot be used to determine the band gap energy.

PACS numbers: 78.66.Fd, 72.80.Ey
Electronic Mail: w_walukiewicz@lbl.gov

Ga-rich InGaN is one of the key materials for short wavelength light emitting devices and has been extensively studied in the past ten years [1]. Much less is known about the In-rich side of this alloy system. Recent measurements of InN crystals grown by the molecular beam epitaxy (MBE) [2,3] or metal-organic vapor phase epitaxy [4] have shown that the bandgap energy of InN is only about 0.7 eV. This value is much smaller than the gap of about 2 eV determined in earlier studies on sputtered InN films [5,6]. The low value of the bandgap of InN results in a large $k \cdot p$ interaction and a strongly non-parabolic conduction band [7]. Further, it has been also shown that the energy gap of InGaN ternary alloys is continuously tunable over a wide spectral range reaching from the near infrared for InN to the near ultraviolet for GaN [8-10].

The temperature dependence of the bandgap is one of the fundamentally and technologically important characteristics of a semiconductor. The existing reports on the temperature dependence of the newly revealed band gap of InN were based on measurements of photoluminescence spectra at different temperatures [3,10]. These results have to be interpreted with caution since the emission spectra measured by photoluminescence spectroscopy originate from localized states in the band tail. Also, the line-shape of the emission spectra can depend on the temperature and the free electron concentration.

In this letter we report the results of studies of the fundamental bandgap of InN as a function of temperature using photoluminescence and optical absorption spectroscopies. We find that only optical absorption provides a reliable method to determine the band gap at low temperatures. The temperature dependence of the band gap of InN is weaker than for most semiconductors. For a sample with low free electron concentration (n = 3.5×10^{17}cm^{-3}), the bandgap variation between room temperature and low temperature is only 47 meV. The implications of this small temperature coefficient will be discussed.

Two InN films were grown on (0001) sapphire with a GaN buffer layer by molecular-beam epitaxy [11]. The thickness of the buffer layer is between 220 - 260 nm. The InN layer thickness is 7.5 μm for both films. Sample A was not intentionally doped, with a free electron concentration of 3.5×10^{17} cm^{-3} and a high carrier mobility of 2050 cm^2/Vs measured by Hall Effect. Sample B was doped with Si. Its free electron concentration and mobility were measured to be 1.2×10^{19} cm^{-3} and 1070 cm^2/Vs,

respectively. Considering their distinctively different doping concentrations and small compensation ratios (indicated by the high carrier mobilities), films A and B can be used as representative samples to study the intrinsic and extrinsic behaviors of the bandgap of InN, respectively. The details of the growth process have been published elsewhere [11].

Samples A and B were characterized by conventional optical absorption experiments and photoluminescence (PL) spectroscopy. The optical absorption measurements were carried out using a liquid-nitrogen cooled Judson photovoltaic InSb detector and a tungsten-halogen lamp dispersed by an ISA HR320 monochromator as the light source. Combining the efficiencies of the detector and the monochromator grating, the system has been tested and it shows a reasonably flat response in the relevant photon energy range from 0.5 to ~ 1.0 eV. The temperature was varied from 12 K to 295 K using a CTI cryogenic system equipped with a Lakeshore auto-tuning temperature controller. The PL signals were generated in the backscattering geometry by excitation with the 476.5 nm line of an argon laser and were dispersed by a 1 m double-grating monochromator.

Figure 1 shows typical absorption spectra of sample A obtained at several different temperatures. The absorption coefficient of these films calculated based on their thickness is on the order of 10^4 cm^{-1} at energies about 0.5 eV above the bandgap, which is a typical value of the absorption coefficient for direct-bandgap semiconductors. The Febry-Perot oscillations observed below the absorption edge indicate high-quality parallel surfaces.

The absorption curve shows a diffusive shape with a strong band tailing effect especially at high temperatures. The diffusive lineshape of the absorption is attributed to the carrier-photon interaction and the carrier-impurity interaction, both increasing with temperature, and the temperature-independent structural disorder effect [12]. A Sigmoidal equation can be used to describe the spectral dependence of the absorption [13],

$$\alpha(E) = a_0 \Big/ \left[1 + \exp\left(\frac{E_g - E}{\Delta} \right) \right], \qquad (1)$$

where E_g is the effective bandgap and Δ is the Urbach broadening factor.

In Fig. 1 the solid curves represent numerical fits to the absorption data based on Eq.(1). To compare the temperature behavior of absorption and emission, we have also performed PL experiments on the same sample in a similar temperature range. Shown in Fig. 2 are representative PL spectra (log scale) excited with a constant laser power (~ 7 mW) at several temperatures. The integrated intensity of the PL signals decreases by ~ 120 times between 15K and room temperature. The full width at half maximum of the PL peak increases from ~ 20 meV to ~ 70 meV. The peak position of the PL shifts to lower energy by ~ 30 meV.

Figure 3 shows the bandgap, the PL peak and the absorption broadening of sample A as a function of temperature. The absorption edge shifts to lower energies by ~ 47 meV as temperature is increased from 12K to room temperature. This change is significantly smaller than that of other group III-nitrides. For example, the change is ~ 72 meV and ~ 92 meV for intrinsic GaN and AlN, respectively [14]. One should note a distinctly different temperature dependence of the PL peak energy. As is seen in Fig. 3 the absorption edge and the PL band gaps differ by as much as 16 meV at low temperature. This difference can be attributed to the fact that the low temperature PL is associated with transitions from low-density localized states whereas the absorption edge is determined by the large-density band states. These results demonstrate that the shift of the PL peak energy cannot be used to determine the temperature dependence of the fundamental band gap of InN.

The temperature dependence of the direct band gap, determined from the absorption edge, can be well described by Varshni's equation [15],

$$E_g(T) = E_g(0) - \frac{\gamma T^2}{T + \beta}. \qquad (2)$$

For the data in Fig. 3 the best fit is obtained with $E_g(0)$=0.69 eV, γ = 0.41 meV/K and β = 454 K. These are compared with the values reported in Ref.[12] on the bandgap observed near 2 eV for a sputter-grown InN film: γ = 0.31 meV/K and β = 580 K. The optical parameters of InN determined in this work are compared with those of GaN and AlN in Table 1. It can be seen that all these parameters show a monotonic chemical trend from AlN to InN. In the Varshni equation, β is physically associated with the Debye temperature of the crystal [15]. The value of β = 454K for InN is consistent with the

calculated range of Debye temperature for InN between 370K and ~ 650K [16]. γ is much smaller than that of GaN and AlN, which suggests that the overall influence of thermal expansion and electron-phonon interaction on the fundamental bandgap is much weaker in InN.

The broadening factor is also plotted in Fig. 3 as a function of temperature. The dependence is linear over the entire temperature range investigated. This broadening is much smaller than the broadening values reported in Ref.[12] obtained on sputtered InN samples. The temperature coefficient of the bandgap is 0.243meV/K at room temperature. It can be decomposed into two parts, *i.e.*, the contribution from the thermal expansion of the lattice structure, and the contribution from the electron-phonon interaction. The former is equal to the product of the pressure coefficient of the bandgap, the bulk modulus, and the thermal expansion coefficient of the lattice constant. Using available literature values of these parameters for InN [3, 17], we have estimated that the contribution of thermal expansion to the temperature coefficient is 0.014meV/K, equal to approximately 6% of the total temperature coefficient observed. Therefore, the temperature coefficient of the bandgap due to the electron-phonon interaction is 0.23meV/K. This compares to the value of 0.29meV/K for GaN, and 0.48meV/K for AlN calculated by the same method.

We have also performed the same measurements on sample B, which has a much higher free electron concentration. Shown in Fig. 4 are the PL peak, absorption edge and broadening parameter as a function of temperature for sample B. The absorption edge in sample B is shifted to higher energy. This is attributable to the Burstein-Moss effect, which is related to different Fermi energies at different doping concentrations [7]. The variation of the absorption edge between room temperature and 12K is 37 meV which is slightly smaller than that of sample A. The parameters of sample B are also listed in Table 1. The large difference between E_g and the PL peak observed in sample B is due to the effect of degenerate doping. The absorption edge energy increases with increasing Fermi level while the emission is still determined by the allowed transitions from the states below the Fermi surface. Also, as is seen in Fig. 4, the PL peak energy exhibits a much weaker, non-monotonic temperature dependence. Again it is evident that the PL measurements cannot be used to obtain the temperature dependence of the bandgap in

InN. The observed significant increase of the bandgap at high doping level indicates that only the results of the unintentionally doped sample can be considered to represent the temperature dependence of the energy gap of intrinsic InN.

In conclusion, we have used optical absorption spectroscopy to measure the temperature dependence of the fundamental bandgap of InN grown by molecular beam epitaxy. The temperature coefficients of a pure InN and a heavily doped InN film have been determined. The bandgap variation with temperature is significantly weaker than those of GaN and AlN. The different temperature behaviors of these two samples were compared and interpreted in terms of the doping effect. The results demonstrate that the position of the PL peak energy is strongly affected by the presence of localized states and cannot be used to determine the temperature dependence of the band gap in InN.

We thank Dr. Henning Feick for his technical help with the spectrometer. This work is supported by the Director, Office of Science, Office of Basic Energy Sciences, Division of Materials Sciences and Engineering, of the U.S. Department of Energy under Contract No. DE-AC03-76SF00098. The work at Cornell University is supported by ONR under Contract No. N000149910936. J. Wu acknowledges support from U.S. NSF Grant No. DMR-0109844.

References

[1] *The Blue Laser Diode*, edited by S. Nakamura and G. Fasol (Springer, Berlin, 1997).

[2] V. Yu. Davydov, *et. al.*, phys. stat. sol. (b) **229**, R1 (2002).

[3] J. Wu, *et. al.*, Appl. Phys. Lett., **80**, 3967(2002).

[4] Tyagai, *et. al.*, Sov. Phys. Semicond. **11**, 1257 (1977).

[5] T. L. Tansley and C. P. Foley, J. Appl. Phys. **59**, 3241 (1986).

[6] Takashi Matsuoka, *et. al.*, Appl. Phys. Lett., **81**, 1246 (2002).

[7] J. Wu, *et. al.*, Phys. Rev. **B 66**, 201403(R) (2002).

[8] J. Wu, *et. al.*, Appl. Phys. Lett., **80**, 4741 (2002).

[9] M. Hori, *et. al.*, phys. stat. sol. (b) **234**, 750 (2002).

[10] V. Yu Davydov, *et. al.*, phys. stat. sol. (b) 234, 787 (2002).

[11] H. Lu, *et. al.*, Appl. Phys. Lett., **79**, 1489 (2001).

[12] W. Z. Shen, *et. al.*, Appl. Phys. Lett., **80**, 2063 (2002).

[13] F. B. Naranjo, *et. al.*, Appl. Phys. Lett., **80**, 231 (2002).

[14] I. Vurgaftman, J. R. Meyer and L. R. Ram-Mohan, J. Appl. Phys., **89**, 5815 (2001).

[15]] H. Teisseyre, *et. al.*, J. Appl. Phys., **76**, 2429 (1994).

[16] V. Yu. Davydov, et. al., Appl. Phys. Lett., **75**, 3297 (1999).

[17] http://www.ioffe.ru/SVA/NSM/Semicond/ and references therein.

Table and Table Captions

Table 1. Bandgap and Varshni parameters of InN measured in this work, and of GaN and AlN adopted from Ref. [13].

parameter	AlN (Ref.[13])	GaN (Ref.[13])	InN, sample A ($n = 3.5\times10^{17}$cm^{-3})	InN, sample B ($n = 1.2\times10^{19}$cm^{-3})
$E_g(0)$ (eV)	6.230	3.507	0.690	0.883
γ (meV/K)	1.799	0.909	0.414	0.481
β (K)	1462	830	454	865
$E_g(0)$-E_g(295K) (meV)	92	72	49	37
dE_g/dT at 295K (meV/K)	0.58	0.42	0.24	0.21

Figure Captions

Fig. 1 Absorption of sample A measured over a wide range of temperatures. The solid curves are fits to the absorption data using Eq.(1).

Fig. 2 PL spectra of sample A measured at different temperatures. The PL intensity is plotted on a log scale.

Fig. 3 PL peak energy, bandgap, and broadening factor of sample A as a function of temperature. The solid curve through E_g is a fit using Eq.(2).

Fig. 4 PL peak energy, bandgap, and broadening factor of sample B as a function of temperature.

Figures

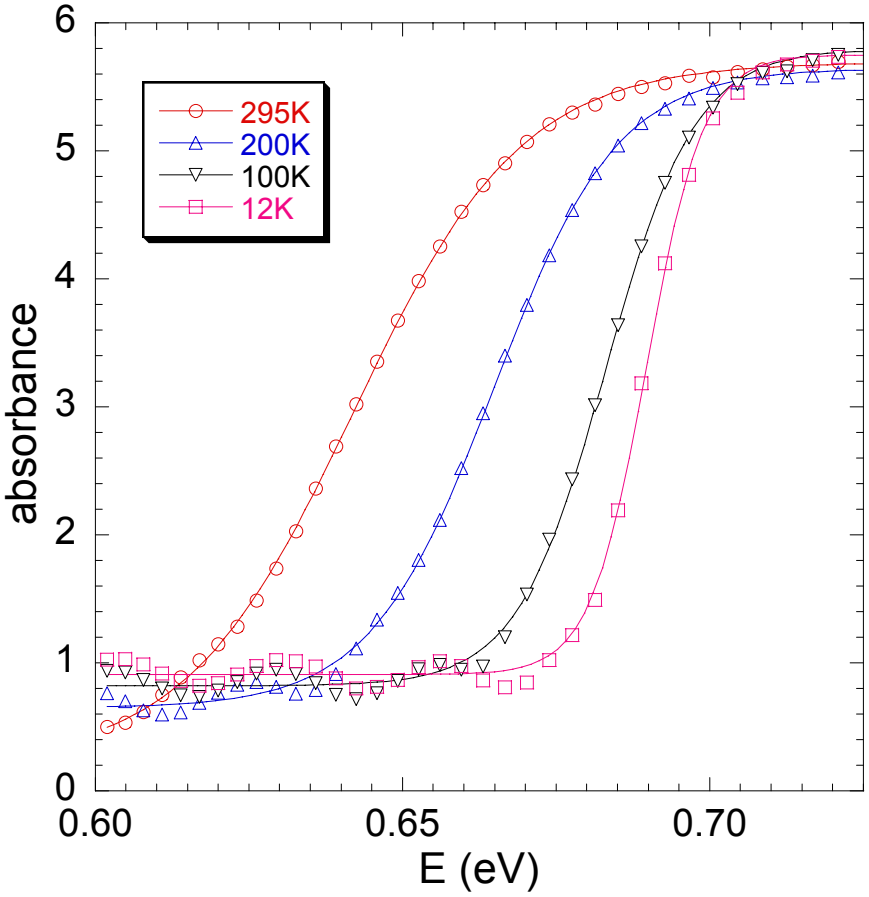

Fig. 1 of 4

J. Wu et. al.

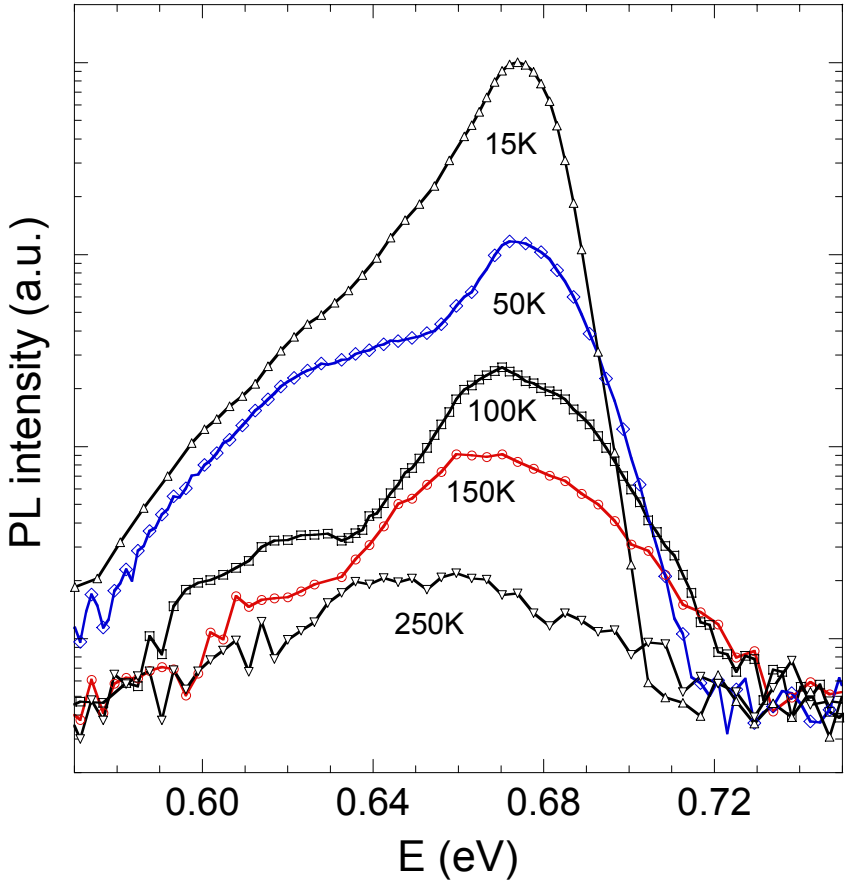

Fig. 2 of 4

J. Wu et. al.

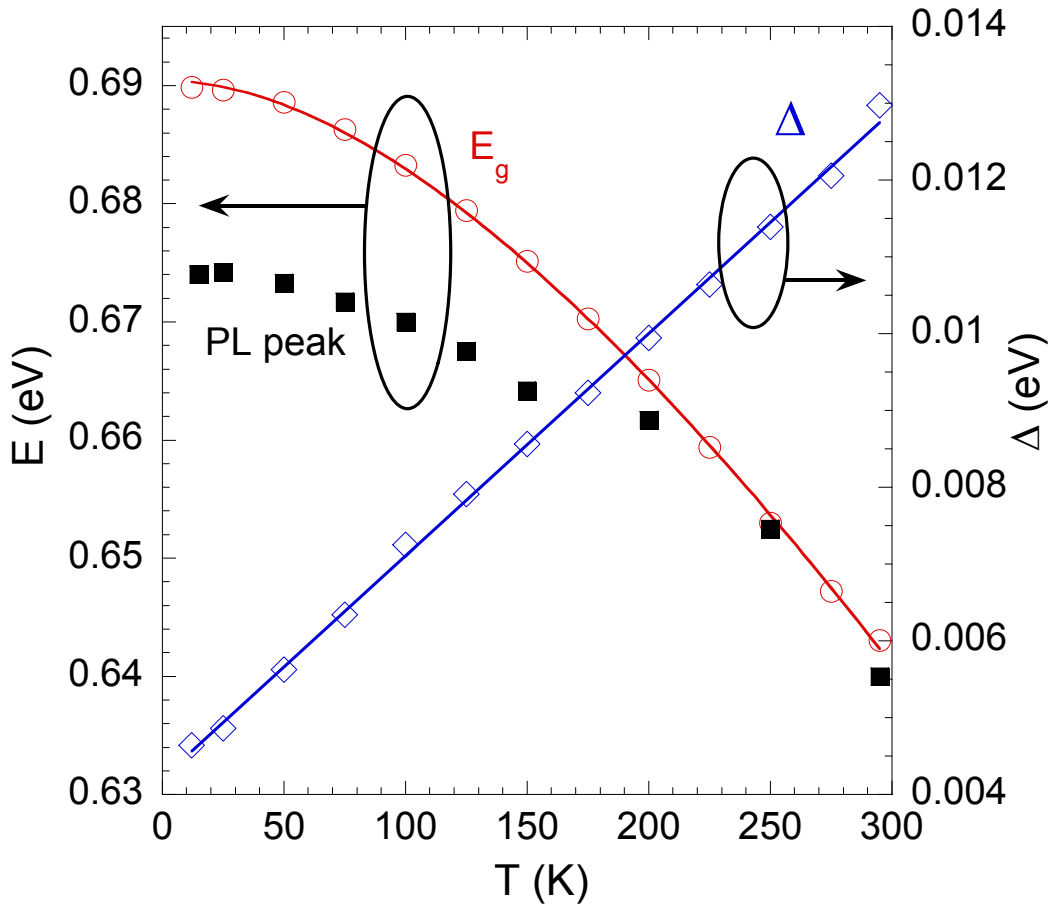

Fig. 3 of 4

J. Wu et. al.

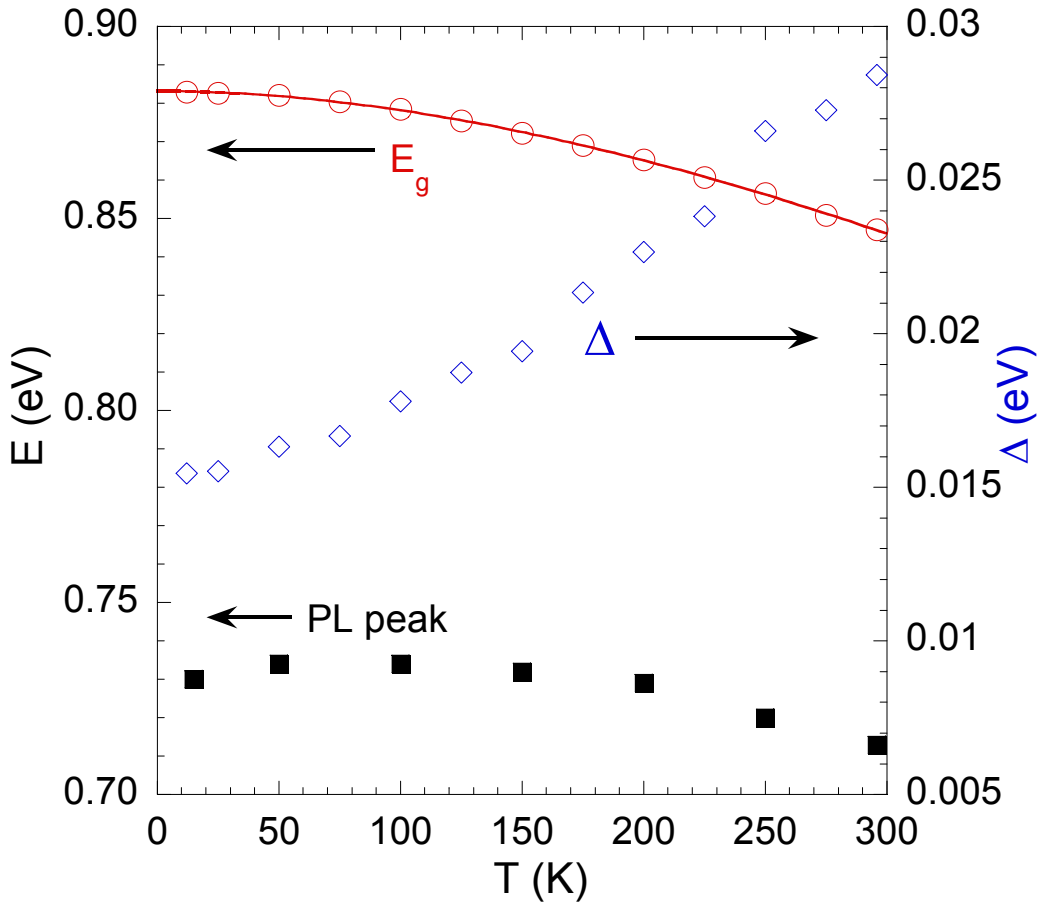

Fig. 4 of 4

J. Wu et. al.